

This article was downloaded by:

On: 18 January 2011

Access details: *Access Details: Free Access*

Publisher *Taylor & Francis*

Informa Ltd Registered in England and Wales Registered Number: 1072954 Registered office: Mortimer House, 37-41 Mortimer Street, London W1T 3JH, UK



International Journal of Environmental Analytical Chemistry

Publication details, including instructions for authors and subscription information:

<http://www.informaworld.com/smpp/title~content=t713640455>

Theoretical Distribution of Silicate in an Urban Sewage Outfall, Correlation with Experimental Data

J. Pérez Peña^a; J. J. Hernández Brito^a; M. González Dávila^a; M. Gelado Caballero^a

^a Faculty of Marine Sciences, Department of Chemistry, Polytechnic University of Canary Islands, Las Palmas, Spain

To cite this Article Peña, J. Pérez, Brito, J. J. Hernández, Dávila, M. González and Caballero, M. Gelado (1989) 'Theoretical Distribution of Silicate in an Urban Sewage Outfall, Correlation with Experimental Data', *International Journal of Environmental Analytical Chemistry*, 37: 1, 63 – 73

To link to this Article: DOI: 10.1080/03067318908026885

URL: <http://dx.doi.org/10.1080/03067318908026885>

PLEASE SCROLL DOWN FOR ARTICLE

Full terms and conditions of use: <http://www.informaworld.com/terms-and-conditions-of-access.pdf>

This article may be used for research, teaching and private study purposes. Any substantial or systematic reproduction, re-distribution, re-selling, loan or sub-licensing, systematic supply or distribution in any form to anyone is expressly forbidden.

The publisher does not give any warranty express or implied or make any representation that the contents will be complete or accurate or up to date. The accuracy of any instructions, formulae and drug doses should be independently verified with primary sources. The publisher shall not be liable for any loss, actions, claims, proceedings, demand or costs or damages whatsoever or howsoever caused arising directly or indirectly in connection with or arising out of the use of this material.

THEORETICAL DISTRIBUTION OF SILICATE IN AN URBAN SEWAGE OUTFALL, CORRELATION WITH EXPERIMENTAL DATA

J. PÉREZ PEÑA, J. J. HERNÁNDEZ BRITO, M. GONZÁLEZ DÁVILA
and M. D. GELADO CABALLERO*

Polytechnic University of Canary Islands, Faculty of Marine Sciences, Department of Chemistry, P.O. Box 550, Las Palmas, Spain

(Received 10 March 1989)

The distribution of molybdate-reactive silicate in the receiving waters of an urban sewage outfall on the coast line has been studied. The relationship between silicate and salinity in the mixing zone shows an almost ideal mixing behaviour on the temporal scale (a few hours) of the dispersion area sampled. The profiles along the depth have shown that the greatest amount of molybdate-reactive silicate is transported in the surface waters, and therefore a two-layer model has been chosen to describe this dispersion. The integrated and average depth isoconcentration lines throughout the dispersion layer have been determined under different oceanographic and meteorological conditions. A numerical transport model based on the advection-diffusion process has been applied in order to explain and predict experimental distributions. Wind, boundary conditions and outfall parameters are used as principal variables, providing the isoconcentration lines for an average integrated distribution in the dispersion layer. The agreement between the theoretical and experimental results is better than 75% for the far field and better than 50% for the near field.

Finally, given these conditions, a conservative behaviour of the silicate can explain the experimental distributions in the mixing zone of an urban sewage outfall within a reasonable margin of error.

KEY WORDS: Silicate, urban sewage, numerical modelling, advection-diffusion.

INTRODUCTION

Since the publication of Sillen's¹ classic paper on the physical chemistry of seawater, a great number of papers have been published dealing with the behaviour of silicates in oceanic and estuarine waters.²⁻⁸ In the estuaries, evidence showing the positive,³ negative⁴⁻⁵ and conservative⁶⁻⁸ correlations of silicate with salinity has been presented. Negative correlations are usually explained taking into account the biological activity (uptake) and interaction with particulate matter, while positive correlations can be understood as additional inputs of silicates from urban sewage outfalls or other anthropogenic dumpings.

*Presented at the 18th International Symposium on Environmental and Analytical Chemistry, Barcelona 5-8 September, 1988.

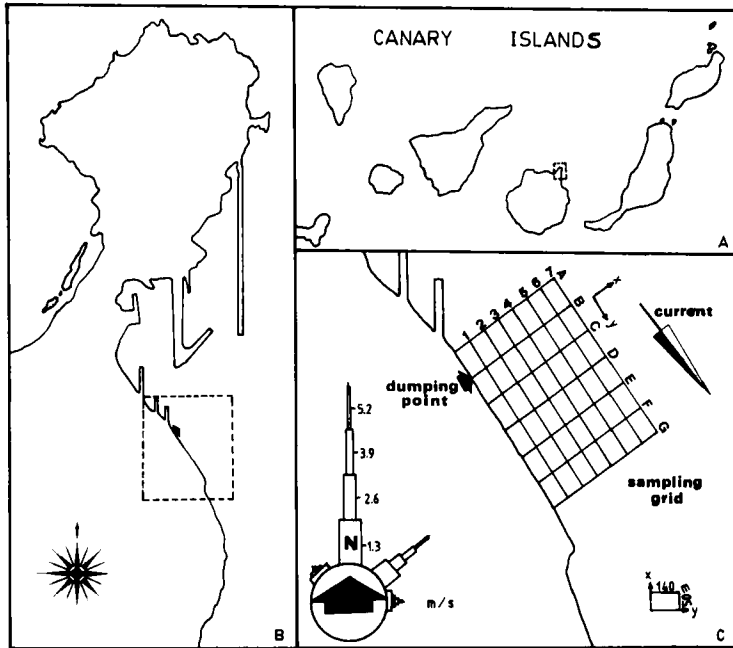


Figure 1 (a)(b) Geographic location of the study area. (c) Sampling grid, compass card, dumping point and prevailing current for the year 1986, reflecting the prevailing Trade Winds.

Depending upon the particular characteristics of a city, the concentration of silicate in urban sewage waters changes and can reach values close to saturation (about $1600\text{--}1800\text{ g at Si l}^{-1}$ at $22\text{--}27^\circ\text{C}$)⁹ in areas rich in basaltic rocks.¹⁰ When the flow of silicate is high enough, these inputs can be a very important factor in the balance of silicate in the estuary. The amount of silicates from these additional sources must be included when the behaviour of silicate is studied, or when the effect of salinity on the concentration of silicates is analyzed.

In the present work, the relationship between silicates and salinity is studied in the mixing zone of an urban sewage outfall, and a model is proposed to compute the isoconcentration lines of a two-dimensional integrated distribution along the depth. Only one source of silicate has been chosen and the dispersion pattern of the same has been modelled in accordance with the behaviour observed.

SAMPLING SITES AND EXPERIMENTAL METHODS

The study area is located in the city of Las Palmas de Gran Canaria (Canary Islands) in the mixing zone of an urban sewage outfall on the coast, with a flow of 70 l/s (Figure 1). The coastline is man-made and rectilinear, while the slope of the sea floor varies in a linear way with the distance from the coast, the depth being 15 m at 350 m from the shore. The material deposited on the sea floor is mainly coarse rock with no organic sediment, except at the dumping point where organic

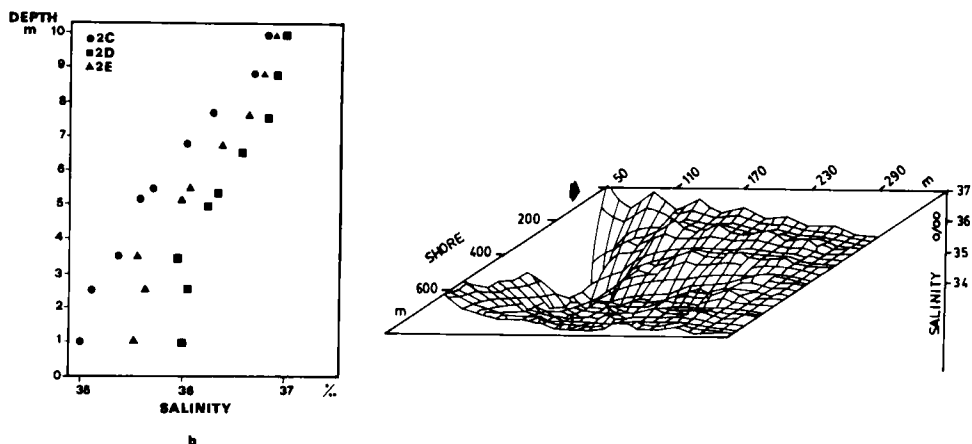


Figure 2 (a) Plot of salinity profiles at different sampling points of the grid. (b) Tridimensional plot of salinity in the mixing zone.

anoxic material has been observed. The sewage is transported by the main current which flows in a S-SE direction, with mean velocities ranging from 2 to 6 cm/s. The Trade Winds prevail, blowing in a NW-NE direction at mean velocities of 3–4 m/s. The sampling grid covers an area of 840×350 square meters, where the separation between the points on the x-axis is 50 m and 140 m on the y-axis, the latter coinciding with the coastline (Figure 1c).

Samples were taken at the knots of this grid under different meteorological conditions and at various depths. Sampling points were determined by 2 theodolites placed along the coast. All the samples were diluted and then filtered through 0.45 μ m acetate cellulose filters. Samples were then stored in polyethylene bottles and frozen at -18°C until their analysis. Dissolved silica ($\text{Si}(\text{OH})_4$) was analyzed in accordance with the procedure recommended by Grasshoff.¹¹ Salinity was measured using a STD sensor mod. Osk315355.

RESULTS

Distribution of Silicates and Salinity

In the mixing zone, the salinity at the surface rapidly changes in the area close to the dumping point, due to the initial dilution. In the far field this variation is less marked (Figure 2a). The variation in salinity from the surface to the bottom shows an exponential shape, with minimum values at the surface (Figure 2b). This superficial layer undergoes greater dilution and therefore transports the greatest amount of the dissolved silicate. The relationship between salinity and silicate concentration is represented in Figure 3. This relationship is observed linear in the dispersion, so the main factor which controls the silicate distribution is the dilution process.

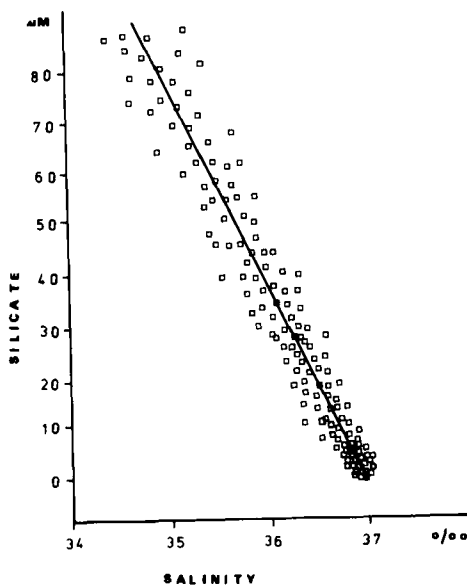


Figure 3 Plot of salinity against silicate in the sampling area. In the range of salinities in the far field, silicate seems to behave as a passive substance.

Based on this fact for this range of salinities, it appears that the behaviour of silicates may approach that of a passive substance, where an almost ideal mixing is achieved. In addition, given the time that the silicate remains in the mixing zone, normally 2–6 hours, the decay due to biological processes does not seem to significantly affect the dissolved silicate concentrations. This type of behaviour has been similarly described for estuaries.

Distribution of Silicate on the Water Column

On the water column, the distribution of silicates presents a two-layer structure; while the larger amount of silicate is found in the upper layer, the concentration near the bottom is very small (Figure 4). The shape of the distribution curve depends on the wind velocity, direction and input conditions. From these results, it may be concluded that silicate transport horizontally is much greater than vertically. This data is confirmed by the configuration of the sea floor, as has been previously described.

It has been observed that for the range of wind velocities studied (2–7 m/s), a percentage of silicates of $90 \pm 3\%$ can be contained in the upper layer as defined by the plane:

$$z = 1.63 \times 10^{-2}x + 3.57 \times 10^{-3}y + 2.3 \quad x, y, z \text{ (m)}. \quad (1)$$

The shape of the distributions curves of the silicate along the depth varies substantially with the wind, but an approximately constant percentage of the total accumulated silicate with the depth is found in this layer.

This plane (Figure 5) divides the water column into two parts; the upper layer transports the pollutant but the lower does not contribute to the dispersion. The dispersion layer has been introduced in order to work out a two-dimensional distribution model of silicates in the water column. The bottom layer contains a

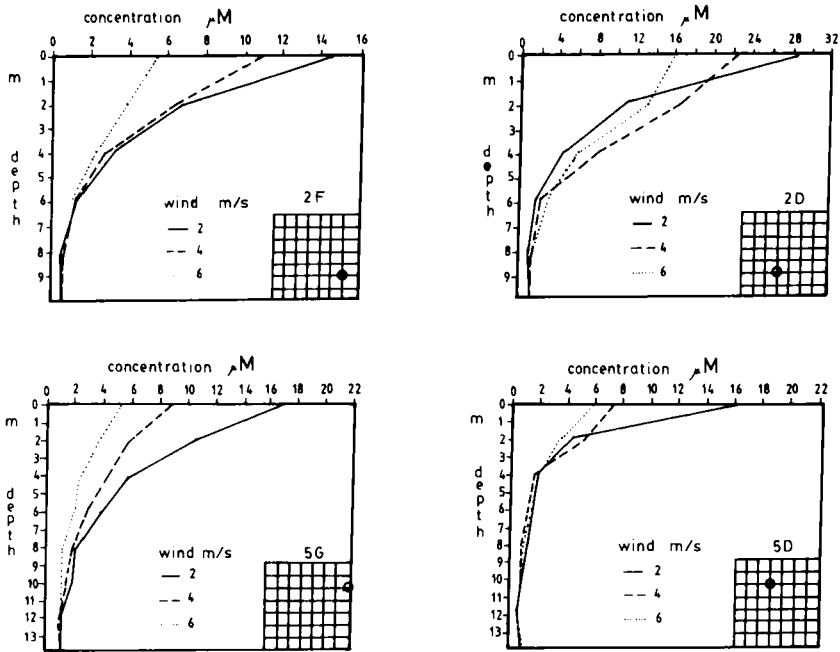


Figure 4 Silicate profiles in the water column para winds blowing of 0°N and velocities of 2, 4 y 6 m/s. The greatest concentrations are found at the surface layer.

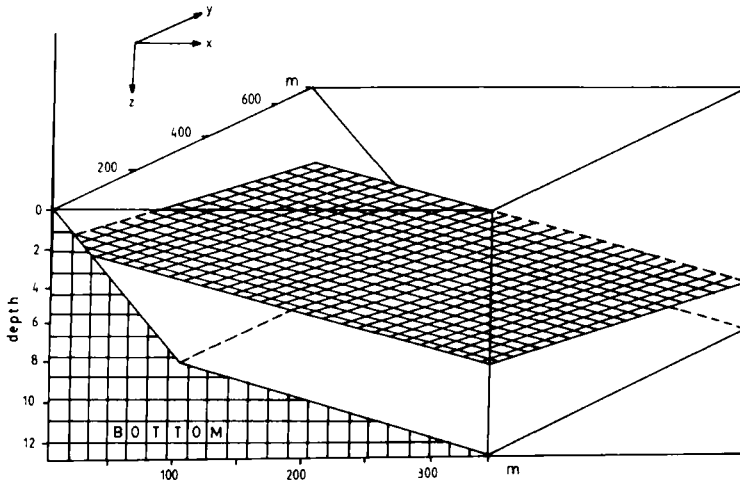


Figure 5 Two-layer model for the distribution of silicate in the water column. The upper layer contains $90 \pm 3\%$ of silicate present in the water column.

very insignificant amount of silicate. The current velocities in this layer are also very low and are strongly affected by the friction with the sea floor. For these reasons, when considering silicate transport and averaging the current velocities, that layer which in fact contains and transports the silicate has been chosen. The currents in this layer are governed mainly by the wind.

Average Integrated Isoconcentration Lines

The concentration of silicate in the dispersion layer defined by Eq. (1) have been integrated for different meteorological conditions at the points of the sampling grid. Concentration at the intermediate points has been interpolated using the one-dimensional advection equation:

$$u \frac{dc}{dx} = k_x \frac{dc}{dx} \quad (2)$$

$$v \frac{dc}{dy} = k_y \frac{dc}{dy} \quad (3)$$

and where the parameters (u, v, k_x, k_y) of same have been evaluated from the initial and final values of the range to be interpolated.

These interpolated data have allowed us to obtain the isoconcentration lines of silicate for an average distribution along the depth (Figure 6). In these figures the effects of wind velocity and direction can be studied. As it can be seen, the isoconcentration lines come near to the dumping point when the wind velocity is increased, as an effect of the increase of the superficial current. As a consequence of the increase of the current, the silicate will be transported faster in the upper layer and the isoconcentration lines come together over the dumping point with respect to the same isoconcentration lines at low current. Also, the isoconcentration gradients in the area close to the outfall are much sharper, demonstrating the effect of the increase advection process. These gradients are less pronounced and the area below the isoconcentration lines widens when the angle formed by the wind and the coastline increases. It is also observed that the distribution axis approaches the coastline in this case. This effect could be explained by taking into account that when this angle increases, the wind-induced current presents a smaller component in the direction of the movement, while the geostrophic current increases due to the build-up of the water mass against the coast.

Model for Computing the Silicate Isoconcentration Lines

These experimental data and distributions have allowed us to construct a transport model based on the advection-diffusion processes generated by wind, assuming that these processes control the silicate distribution. This model impli-

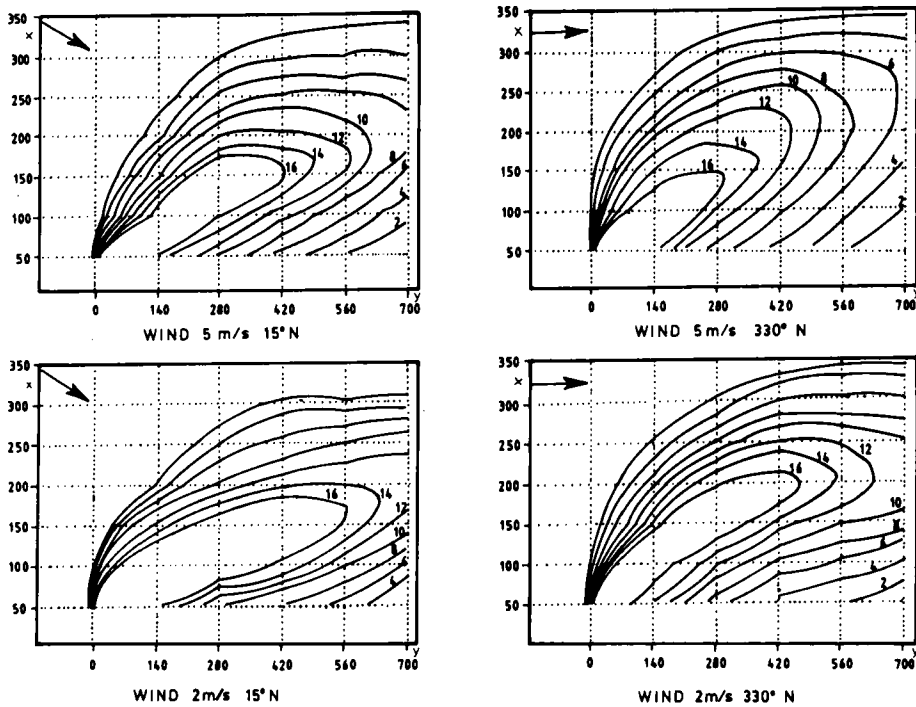


Figure 6 Average integrated isoconcentration lines in the dispersion layer under different meteorological conditions. Silicate distribution is governed mainly by wind velocity and direction.

cityly supposes that the wind-induced currents and pressure gradients are the conductors of the movements of the water mass and therefore of the silicate.

The hypotheses on which the model is based are:

1. The fluid is considered incompressible.
2. The meteorological and oceanographic conditions are considered stationary, as well as the source flow.
3. The dispersion process on the water column occurs in a two-layer structure.
4. The current has been expressed as a combination of the wind-induced and geostrophic currents.
5. The two-dimensional approximation is carried out by integrating the velocity field and concentrations in the layer of water where the dispersion process takes place.
6. The behaviour of the silicate is roughly that of a passive substance for the temporal and spatial scales of the model.
7. It is assumed that there is no transverse flow along the coastline, except at the outfall.

On the basis of these hypotheses, the advection–diffusion equation for the passive pollutants in a two-dimensional distribution can be expressed as:^{12, 13}

$$U \frac{\partial C}{\partial x} + V \frac{\partial C}{\partial y} = k_x \frac{\partial C}{\partial x} + k_y \frac{\partial C}{\partial y} \quad (4)$$

where U and V are the average velocity components of the currents which are parallel and perpendicular to the coast respectively, and K_x and K_y the turbulence coefficients. The two-dimensional components have been obtained by integrating and averaging the velocity field into the dispersion layer. Current velocities on the water column have been obtained as a combination of the current resulting from wind stress and pressure gradients. These components have been obtained from the hydrodynamic equation:¹²

$$2W \sin u = \frac{A}{\rho} \frac{\partial V}{\partial z} - \frac{1}{\rho} \frac{\partial P}{\partial x} \quad (5)$$

$$2W \sin v = \frac{A}{\rho} \frac{\partial U}{\partial z} - \frac{1}{\rho} \frac{\partial P}{\partial y} \quad (6)$$

for the case where the driving force is the wind stress on the surface and coupling between individual layers of water, and for the case where a slope in the surface exists, but no wind is present. It is important to emphasize that the frictional terms of the above equations are included in the calculation of the geostrophic current. The slope of the water surface perpendicular to the coast has been obtained by applying the continuity equation for mass transport:¹⁴

$$\tau = \rho' C_z^* W_z \quad (7)$$

where ρ' is the air density, C_z^* is the coefficient of aerodynamic strength at height z above the sea surface and W_z is the wind velocity at the same level. The value of C_z^* has been fixed as 1.1×10^{-3} providing the best correlations with the experimental results.

The partial derivative equations have been solved using a finite difference method. The advective term has been discretized using the procedure of Stone and Brian,¹⁵ but using a two-dimensional grid extended to six points.

The diffusive term has been discretized using the procedure of Crank-Nicholson.¹⁵ The resulting equations have been solved using an iterative method, where the algorithm has been obtained from discretized advection-diffusion equations.

To solve these equations, a computer program (ADVEC-II) was written in FORTRAN 77 and run in a Micro-Vax II/VMS.

Input for the program includes boundary conditions, wind direction and velocity and concentration at the source. Output provides the induced velocity field and the integrated isoconcentration lines in the dispersion layer within the limits of the simplifications introduced into the model. The printout is obtained from a graphic terminal or plotter.

The coastal condition has been modelled assuming that the concentration

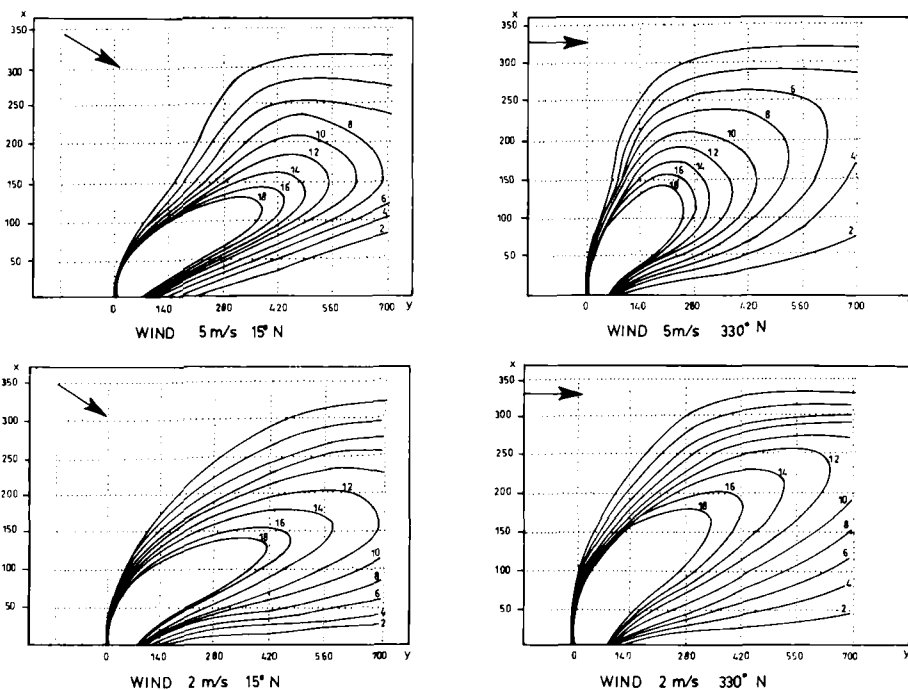


Figure 7 Theoretical isoconcentration lines for a two-dimensional model of the mixing zone under different wind conditions. Experimental data can be modelled based on advection and diffusion processes generated by wind.

gradients are zero, and the ocean boundary conditions have been determined experimentally.

DISCUSSION

The theoretical isoconcentration lines obtained using a flow of 70 l/s and silicate concentration of 1.5 M as outfall parameters are shown in Figure 7 for different meteorological conditions. The correspondence with the experimental results and the same dependence on the theoretical isoconcentration lines with the wind velocity and direction are observed. The increase in wind velocity causes the isoconcentration lines to come together, because transport by advection increases. The flow of silicate leaving the model area increases and therefore, in order to satisfy the balance of material, the isoconcentration lines must be close in on the outfall.

With respect to wind direction, the increase in the component perpendicular to the coast produces an increase in the geostrophic current and more energy is used in the turbulent mixing process than in advective transport. This is shown in Figure 7 as an expansion of the isoconcentration lines. Likewise, as a consequence of the composition of the wind-induced and geostrophic currents, the distribution axis approach the coastline.

The correlation between the theoretical and experimental results is shown in

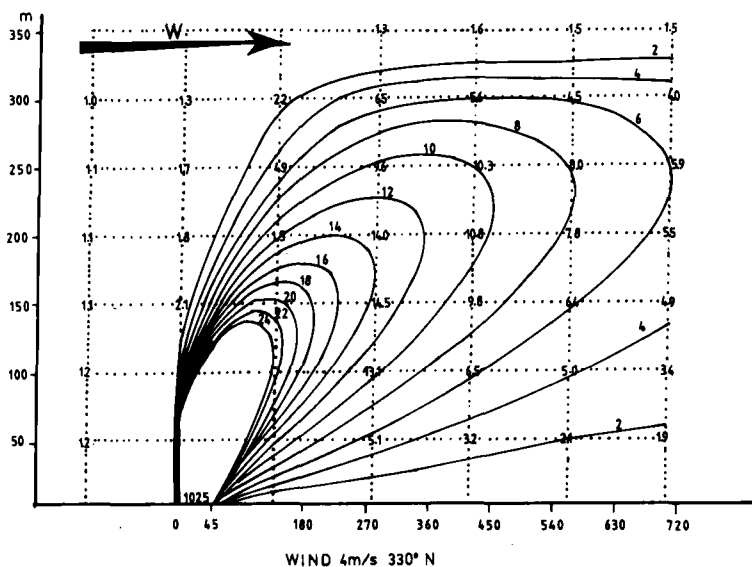


Figure 8 Theoretical isoconcentration lines for wind blowing 0°N and 4 m/s and experimental data plotted in the knot of the grid.

Figure 8 for winds blowing 0°N at 4 m/s. The best correlation is found in the far field, while the agreement is less near the dumping point. This may be attributed to the high concentration gradients present in this area, where at a few meters distance, the concentration may change very sharply. Precision in the determination of sampling sites is crucial and may be a source of error. Thus, accuracy in measuring the samples taken from the same point in this area varies $\pm 5\%$.

Greater agreement in the far field is found, where the theoretical results confirm the experimental ones, within a margin of error less than 25%. Systematic variations in the theoretical values are not significant in the far field and thus the possible sources of error have been introduced into the model, since wind direction and velocity do not remain stationary.

The inclusion of time in the model could complicate the mathematical treatment, while our aim was to construct a simple model which might be valid in statistical rather than deterministic terms.

In conclusion, the working hypotheses are valid within a margin of error of 25%, the greatest cause of error coming from the stationary hypothesis. The behaviour of silicates under the conditions studied can be explained principally by taking into consideration the transport processes controlled by diffusion and advection.

References

1. L. G. Sillen. In: *Oceanography* (M. Sears, ed.) (AAAS, Washington, D.C., 1961), pp. 540–545.
2. H. L. Simpson, D. E. Hammond, B. L. Deck and S. C. Williams. In: *Marine Chemistry in the Coastal Environment* (T. M. Church, ed.), ACS Symposium Series 18 (1975).

3. E. Boyle, R. Collier, A. T. Dengler, J. M. Edmond, A. G. Ng and R. T. Stallard, *Geochim. Cosmochim. Acta*, **38**, 1719 (1974).
4. P. S. Liss and C. P. Spencer, *Geochim. Cosmochim. Acta*, **34**, 1073 (1970).
5. J. D. Burton, *J. Cons. Int. Explor. Mer.* **33**, 141 (1970).
6. H. Maeda and K. Takesue, *Rec. Oceanogra. Wks. Japan* **6**, 112 (1961).
7. U. Stefansson and F. A. Richards, *Limnol. Oceanogr.* **8**, 394 (1963).
8. J. J. Ryther, D. W. Menzel and N. Corwin, *J. Mar. Res.* **25**, 69 (1967).
9. K. B. Krauskopf, *Geochim. Cosmochim. Acta* **10**, 1 (1956).
10. H. D. Holland ed., *The Chemistry of the Atmosphere and Oceans* (John Wiley and Son, 1978).
11. K. Grasshoff, M. Erhardt and K. Kremling, eds., *Methods of Seawater Analysis*, 2nd edn. (Winheim, Verlag Chemie, 1983).
12. G. Kulleberg. In: *Pollutant Transfer and Transport in the Sea* (CRC Press Inc., 1982), Vol. 1.
13. S. S. Park. In: *Mathematical Modeling of Mixing Zone Characteristics in Natural Streams*, Ph.D. Thesis (Rutgers University, The State University of New Jersey, 1985).
14. G. Neumann and W. J. Pierson. In: *Principles of Physical Oceanography* (Prentice-Hall, Inc., Englewood Cliffs, New York, 1966).
15. B. W. Wilson, *J. Geophy. Reser.* **65** (10) 3377 (1960).
16. H. G. Ramming and Z. Kowalik. In: *Numerical Modelling of Marine Hydrodynamic. Applications to the Dynamic Physical Processes* (Elsevier Oceanography Series, 1980).
17. H. P. Stone and P. L. T. Brian, *J. Amer. Inst. Chem. Engin.* 681 (1963).
18. J. Crank and P. Nicholson, *Proc. Cambridge Phi. Soc.* **43**, 50 (1947).